Cold agglutination as a pivotal diagnostic clue for Waldenström macroglobulinemia: A rare case report with diagnostic and therapeutic insights

WEI ZHANG[1*], YONGWU XIA[1*], ZIHUA YANG[2], LIUBING ZHANG[1], XIAOXIN JIANG[1], TING CAI[3] and PINGHONG MING[1]

[1]Department of Clinical Laboratory, The People's Hospital of Longhua, Shenzhen, Guangdong 518109, P.R. China; [2]Department of Clinical Laboratory, Shenzhen People's Hospital, Shenzhen, Guangdong 518020, P.R. China; [3]Department of Acupuncture and Moxibustion, The First Affiliated Hospital of Shenzhen University, Shenzhen, Guangdong 518055, P.R. China

Received December 17, 2025; Accepted April 23, 2026

DOI: 10.3892/etm.2026.13212

Abstract. Waldenström macroglobulinemia (WM) is a rare indolent B-cell lymphoproliferative disorder characterized by bone marrow infiltration and monoclonal immunoglobulin M (IgM) secretion, which poses diagnostic challenges in the early stage. The present study reported on a 63-year-old male with WM presenting with cough, hyperviscosity syndrome (dizziness, weakness, fatigue, blurred vision), severe anemia and cold agglutination in August 2023. After 37˚C incubation to eliminate cold agglutination interference, laboratory tests confirmed severe anemia (hemoglobin, 54 g/l), hyperglobulinemia (globulin, 92 g/l) and markedly elevated serum IgM (83.6 g/l). Peripheral blood smear showed erythrocyte rouleaux formation and plasmacytoid lymphocytes. Bone marrow biopsy revealed 80% infiltration of B-lymphomatous cells, 10% abnormal plasma cells and only 10% residual normal hematopoietic cells. Serum/urine immunoelectrophoresis identified IgM-λ paraprotein and free λ light chains. Bone marrow flow cytometry detected a prominent abnormally mature B-lymphocyte population (72.2% of lymphocytes) positive for CD19, CD20 and cytoplasmic λ (cλ); partially positive for CD23, CD25 and CD27; and negative for CD5, CD10 and CD103. Abnormal plasma cells (0.3% of nucleated cells) showed cλ restriction; strong expression of CD38, CD138 and CD19; partial expression of CD20 and CD27; and absence of CD5, CD10 and CD56. Genetic testing confirmed the MYD88 innate immune signal transduction adaptor (MYD88) L265P mutation positivity via allele-specific PCR and 14q32/11q13 translocation negativity using fluorescence *in vitro* hybridization, confirming the diagnosis of WM. The patient received therapeutic plasma exchange (TPE) followed by bortezomib-dexamethasone chemotherapy, resulting in resolved cold agglutination, alleviated hyperviscosity syndrome and improved laboratory indicators. Follow-up was performed immediately after discharge; however, it was terminated after 1 month (November 2023) due to re-admission for pulmonary infection. In conclusion, cold agglutination is a pivotal diagnostic clue for WM; combined immunophenotyping and MYD88 L265P detection enables definitive diagnosis, and early TPE plus chemotherapy effectively ameliorates clinical manifestations.

Introduction

Lymphoplasmacytic lymphoma (LPL)/Waldenström's macroglobulinemia (WM) is a rare indolent B-cell lymphoproliferative disorder (B-LPD), characterized by clonal lymphoplasmacytic proliferation in the bone marrow and massive secretion of monoclonal immunoglobulin M (IgM) (1). WM accounts for 90-95% of all LPL cases, predominantly affecting the elderly population with an annual incidence of ~3 per million adults (2-4). Clinical manifestations are heterogeneous, with nearly 30% of patients being asymptomatic initially at early stages and do not require immediate treatment (1). By contrast, symptomatic patients may present with a variety of signs, the most common of which include fatigue and anemia caused by bone marrow infiltration (1). However, certain patients develop hepatosplenomegaly, lymphadenopathy or life-threatening hyperviscosity syndrome characterized by dizziness, fatigue, weakness and blurred vision (1). Due to its insidious onset and non-specific initial symptoms, numerous patients first present to non-hematology departments, leading to diagnostic delay

Correspondence to: Dr Ting Cai, Department of Acupuncture and Moxibustion, The First Affiliated Hospital of Shenzhen University, 2 Zhenhua Road, Shenzhen, Guangdong 518055, P.R. China
E-mail: caiqiju@126.com

Dr Pinghong Ming, Department of Clinical Laboratory, The People's Hospital of Longhua, 38 Jianshe Road, Shenzhen, Guangdong 518109, P.R. China
E-mail: mph711@outlook.com

*Contributed equally

Key words: Waldenström macroglobulinemia, cold agglutination, hyperglobulinemia, MYD88 L265P mutation, therapeutic plasma exchange, chemotherapy

and compromised prognosis (5). Therefore, identifying early, recognizable diagnostic clues is critical.

A major diagnostic challenge lies in WM's overlapping features with other mature B-LPDs and the lack of distinctive early warning signs. Cold agglutination-an uncommon but insightful laboratory clue-rarely receives routine clinical emphasis. Pathogenic cold agglutinins in WM are mostly monoclonal IgM antibodies targeting erythrocyte I/i antigens, inducing spontaneous agglutination at room or lower temperatures. Cold agglutination not only triggers autoimmune hemolytic anemia via high-titer monoclonal IgM binding to erythrocyte I/i antigens but also severely distorts routine hematological test results, mimicking primary autoimmune hemolytic anemia or idiopathic cytopenia (6,7). This laboratory interference readily leads to misdiagnosis and delays recognition of the underlying WM. Given that WM cases presenting with cold agglutination as the inaugural and pivotal diagnostic clue are rare, this misdiagnosis risk is amplified, underscoring the critical need for heightened clinical and laboratory awareness of this atypical presentation (6).

Definitive WM diagnosis requires excluding other B-LPDs via integrated clinical, histopathological, laboratory, immunophenotypic and genetic data (4,8-10). Core criteria include bone marrow lymphoplasmacytic infiltration, serum monoclonal IgM elevation, characteristic immunophenotypic profiles by flow cytometry (FCM) and the highly specific MYD88 innate immune signal transduction adaptor (MYD88) L265P mutation (2,4,11). For patients presenting with marked IgM elevation (>40 g/l) and severe hyperviscosity syndrome, therapeutic plasma exchange (TPE) is the first-line emergency intervention to rapidly reduce circulating IgM levels, followed by bortezomib-dexamethasone chemotherapy to control the underlying clonal proliferation (1,12). The present study reported on a 63-year-old male patient with WM where cold agglutination-induced test interference served as the decisive initial diagnostic clue. Through integration of systematic laboratory assessments, immunophenotyping and genetic analyses, the diagnosis of WM was confirmed. Due to the markedly elevated IgM (>40 g/l) and hyperviscosity syndrome, emergency TPE was implemented as the initial intervention, followed by bortezomib plus dexamethasone chemotherapy, achieving satisfactory clinical outcomes. This case highlights cold agglutination as a pivotal diagnostic clue for WM, emphasizes that integrating cellular immunophenotyping with MYD88 L265P mutation detection is critical for definitive diagnosis and validates that early sequential plasma exchange and chemotherapy effectively improve clinical manifestations in such patients.

Case report

Case presentation. A 63-year-old man was admitted to the Department of Hematology, People's Hospital of Longhua (Shenzhen, China) in August 2023, presenting with cough, dizziness, weakness, fatigue, blurred vision and severe anemia. The symptoms had worsened (dizziness and fatigue) with paroxysmal cough and expectoration following an upper respiratory tract infection 1 month prior. An ophthalmological consultation due to blurred vision confirmed bilateral retinal hemorrhage, bilateral macular edema and bilateral ametropia. After a series of examinations, the patient was diagnosed with WM. Owing to the patient's concerns about treatment efficacy, he was transferred to the Department of Hematology, Shenzhen People's Hospital (Shenzhen, China) for further treatment. The patient was managed with a stepwise strategy of symptomatic plasma exchange followed by bortezomib plus dexamethasone chemotherapy, resulting in satisfactory clinical symptom remission and resolution of cold agglutination.

Diagnostic workup. Upon admission, a series of laboratory examinations were performed to make a definite diagnosis. Of note, initial hematology analysis triggered a clot detection alarm, with the EDTA-anticoagulated blood specimen showing fine sand-like erythrocyte agglutination adherent to the tube wall (Fig. 1A). Following centrifugation, the serum stored at 4˚C rapidly formed semisolid gel-like aggregates (Fig. 1B), which gradually liquefied at room temperature (~25˚C) (Fig. 1C), confirming severe cold agglutination.

To eliminate the interference of cold agglutination and obtain valid hematological parameters, the specimens were incubated at 37˚C for 30 min and analyzed immediately. Key findings included severe anemia, as evidenced by a decreased red blood cell count ($1.73x10^{12}$/l; reference range: 4.1-5.8$x10^{12}$/l), hemoglobin concentration (54 g/l; reference range: 125-174 g/l), hematocrit (17.4%; reference range: 40-50%), white blood cells ($5.1x10^{9}$/l; reference range: 3.5-9.5) and platelets ($109x10^{9}$/l; reference range: 125-350$x10^{9}$/l). The biochemical analysis revealed markedly elevated total protein (131 g/l; reference range: 63-82 g/l), globulin (92 g/l; reference range: 24-35 g/l), hypercalcemia (serum Ca^{2+}: 3.15 mmol/l; reference range: 2.1-2.69 mmol/l) and impaired renal function [creatinine (143 μmol/l; reference range: 58-110 μmol/l); creatinine clearance (45 ml/min; reference range: >80 ml/min)]. Additional abnormalities included elevated β2-microglobulin (6.16 mg/l; reference range: 1.3-3.0 mg/l); 24-h urinary total protein (24-UMTP) (1,018.8 mg/24 h; reference range: 50-80 mg/24 h), markedly elevated IgM (83.6 g/l; reference range, 0.3-2.2 g/l), decreased IgG (6.05 g/l; reference range, 8.6-17.4 g/l) and IgA (0.55 g/l; reference range, 1.0-4.2 g/l).

Given the markedly elevated serum IgM level, serum protein electrophoresis was performed via capillary electrophoresis using the HYDRAGEL PROTEIN(E) kit (cat. no. PN4140; Sebia) according to the manufacturer's protocol, which demonstrated an elevated γ-globulin fraction (61.3% of total protein) and a distinct monoclonal protein peak accounting for 53.2% of the γ-globulin fraction (Fig. 2A). The agarose gel immunofixation electrophoresis using the HYDRAGEL IF kit (cat. no. PN4309; Sebia) according to the manufacturer's protocol to further identified the monoclonal component as IgM-λ in the serum (Fig. 2B). In addition, urine protein components were analyzed by agarose gel immunofixation electrophoresis using the aforementioned HYDRAGEL IF kit. Distinct precipitation bands were detected in both the λ light chain and free λ light chain lanes (Fig. 3A), indicating positive urine Bence-Jones protein of the free λ light chain type. Urine immunofixation electrophoresis also revealed an abnormal monoclonal band in the λ lane, indicating that the monoclonal immunoglobulin was of the free λ light chain type (Fig. 3B). All electrophoresis experiments were performed on the Sebia HYDRASYS 2

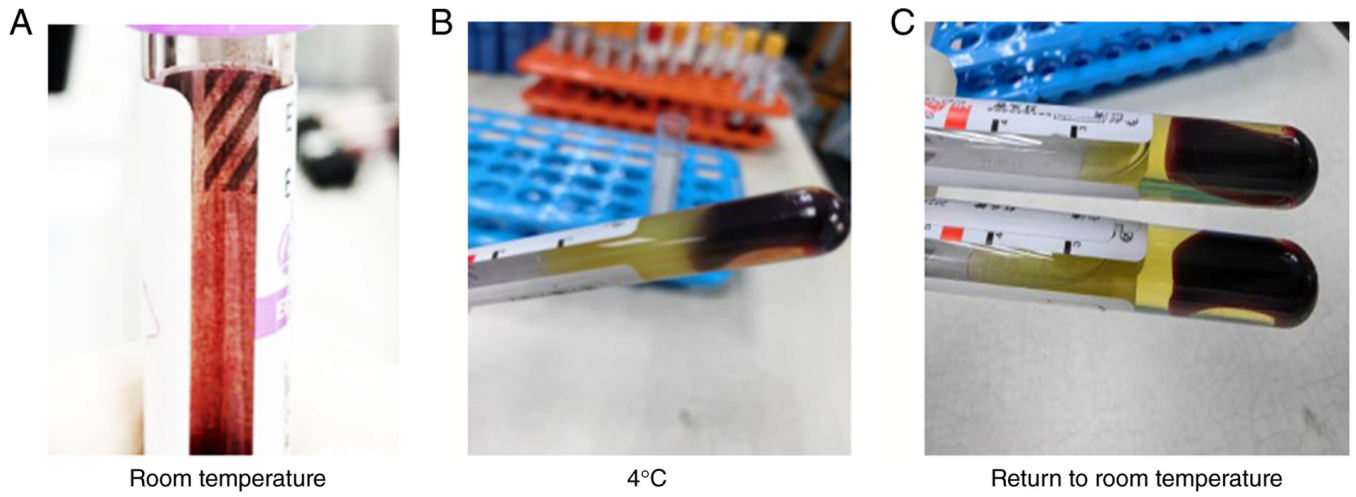

Figure 1. Cold agglutination phenomenon of specimens. (A) Fine sand-like erythrocyte aggregates on the inner wall of EDTA-anticoagulated blood tubes. (B) Serum solidified into a gelatinous mass after 4˚C incubation. (C) Serum liquefaction after rewarming at room temperature.

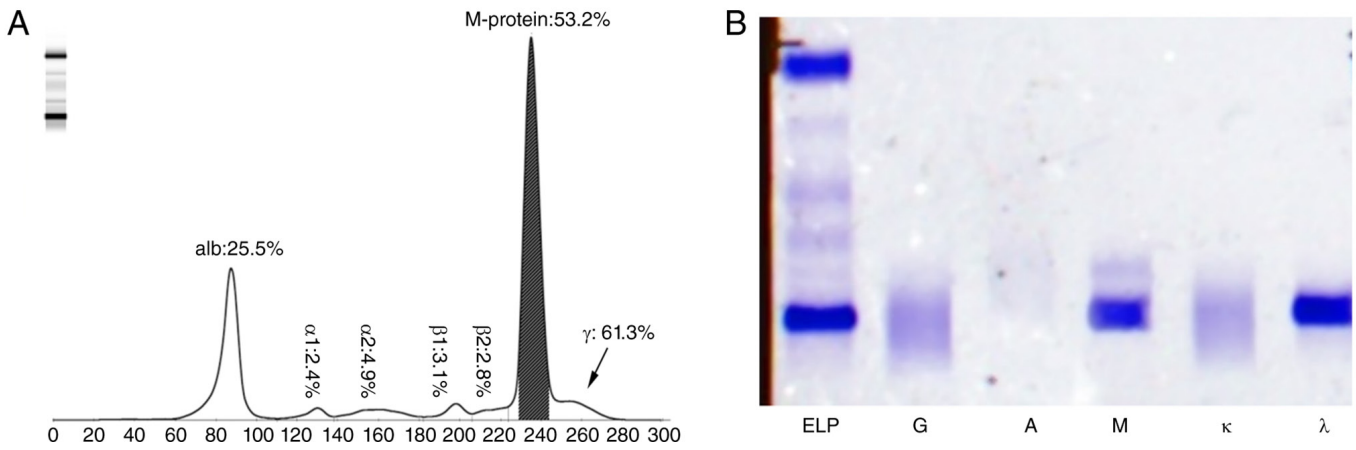

Figure 2. Serum protein electrophoresis and immunofixation electrophoresis. (A) Serum protein electrophoresis showing a distinct monoclonal protein peak in the γ-globulin region, accounting for 53.2%. (B) Immunofixation electrophoresis confirming the component of monoclonal protein as IgM-λ. ELP, electrophoresis lane; G, immunoglobulin G; A, immunoglobulin A; M, immunoglobulin M; κ, κ light chain; λ, λ light chain.

SCAN FOCUSING automated electrophoresis system (Sebia) in accordance with the manufacturer's reagent protocols.

Morphological examination is a crucial approach for evaluating hematological disorders (8). In the present study, Wright-Giemsa staining (Solution A, cat. no. BA4017C; Solution B, cat. no. BA4017D; Baso Diagnostics Inc.) was performed to assess the morphology of peripheral blood and bone marrow specimens, according to the manufacturer's protocol. Briefly, smears were stained with solution A for 1 min, mixed with solution B and incubated at room temperature for 3-10 min. After rinsing and air-drying, the smears were examined under a light microscope with x100 oil immersion. Peripheral blood smear showed rouleaux formation and atypical lymphocytes (Fig. 4A). Bone marrow cytology also demonstrated rouleaux formation and an increased lymphocyte proportion with frequent plasmacytoid lymphocytes (Fig. 4B). Furthermore, hematoxylin and eosin (H&E) staining was used to evaluate the cellular morphology of bone marrow biopsy specimens. Briefly, specimens were fixed in 10% formalin for 12 h at room temperature, embedded in paraffin and cut into 5-μm section. The sections were then deparaffinized (xylene I: 5 min; xylene II: 5 min), hydrated through graded ethanol (100% for 3 min, 90% for 3 min, 80% for 2 min and 70% for 2 min), stained with hematoxylin for 5 min, differentiated in 1% hydrochloric alcohol for 3 sec, blued in tap water for 15 min, counterstained with 0.5% eosin for 10-15 sec, dehydrated through graded ethanol (80% for 5 sec, 90% for 15 sec, 95% for 30 sec and 100% for 5 min), cleared in xylene (xylene I: 5 min; xylene II: 5 min) and mounted with neutral balsam; all at room temperature. Morphological observation was carried out using an Olympus BX53 microscope (Olympus Corporation). It revealed focal collagenous fibrosis of the medullary stroma, a diffuse lymphocytic infiltrate exhibiting plasma cell differentiation and small clusters or focal aggregates of plasma cells. The bone marrow was extensively infiltrated by B-cell lymphomatous cells, which accounted for ~80% of nucleated cells, while abnormal plasma cells comprised 10%, with only 10% residual normal hematopoietic elements remaining (Fig. 4C). These morphological features are consistent with B-cell

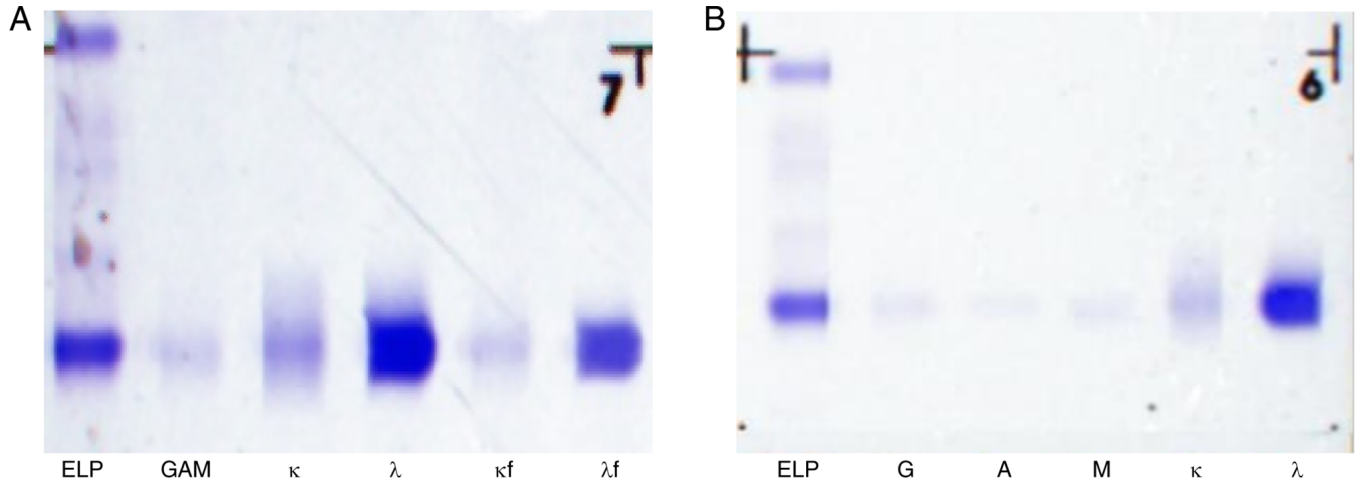

Figure 3. Urine Bence Jones protein electrophoresis and immunofixation electrophoresis. (A) Distinct monoclonal bands in the λ and free λ light chain lanes indicate clonal proliferation of monoclonal λ light chains (including free light chains) in urine. (B) A monoclonal band in the λ light chain lane confirms the presence of urinary monoclonal λ light chains. ELP, electrophoresis lane; GAM, mixed immunoglobulin G/A/M; G, immunoglobulin G; A, immunoglobulin A; M, immunoglobulin M; κ, κ light chain; λ, λ light chain; κf, κ free light chain; λf, λ free light chain.

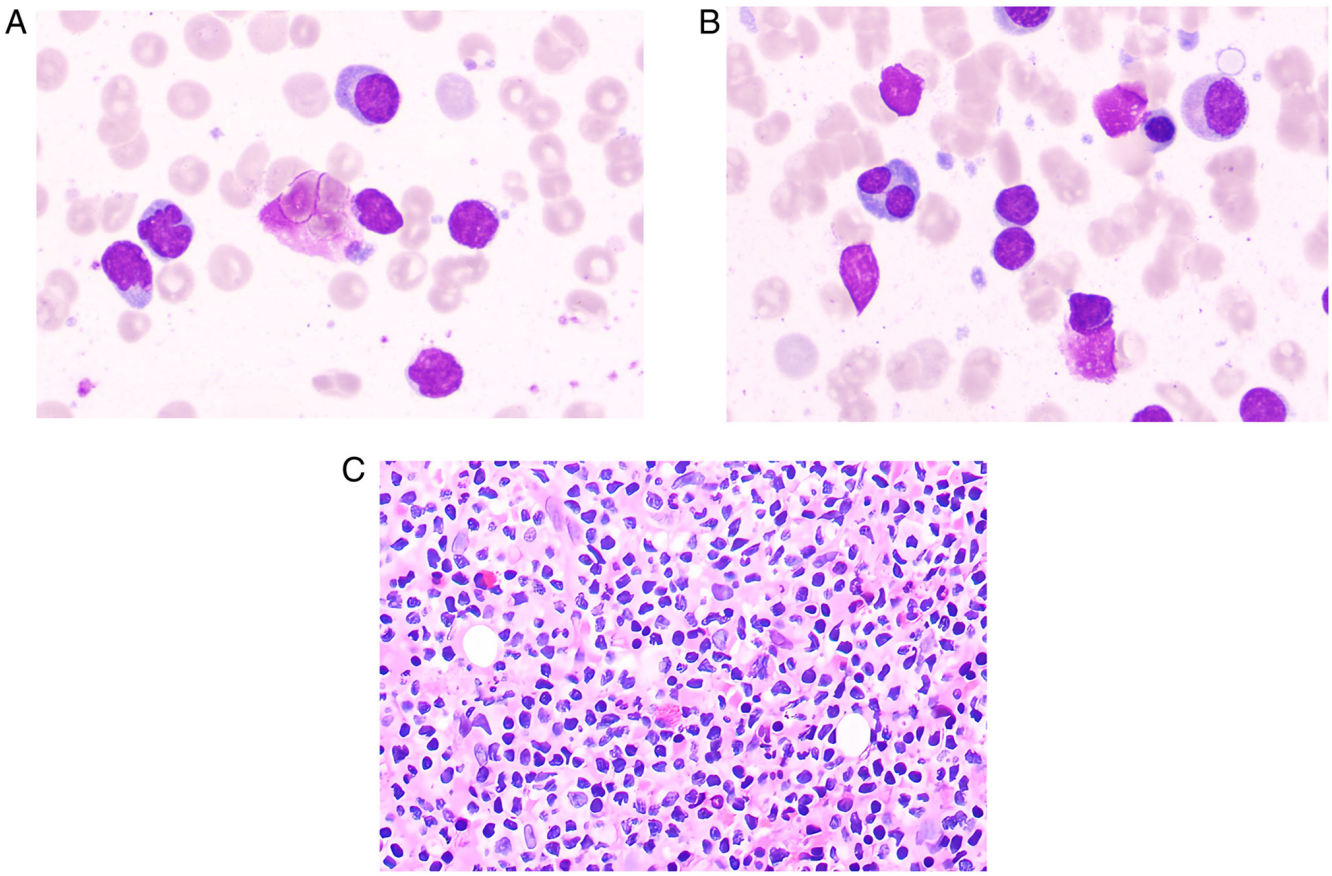

Figure 4. Morphological examination of peripheral blood and bone marrow. (A) Peripheral blood smear showing erythrocyte rouleaux formation and plasmacytoid lymphocytes (Wright-Giemsa staining; magnification, x1,000). (B) Bone marrow cytology showing erythrocyte rouleaux formation and increased plasmacytoid lymphocytes (Wright-Giemsa staining; magnification, x1,000). (C) Bone marrow biopsy revealing diffuse infiltration of lymphocytes with plasmacytoid differentiation (H&E staining; magnification, x400).

lymphoma, which is characterized by lymphoplasmacytic infiltration and suppression of normal hematopoiesis (1,8).

To identify the specific B-cell lymphomatous subtype, immunophenotyping by FCM was performed on bone marrow cells (13-15). Fresh bone marrow aspirate (anticoagulated with EDTA) was subjected to red blood cell lysis (BD Pharm Lyse™; cat. no. 555899; BD Biosciences) and mononuclear cells were resuspended in PBS at $1x10^6$ cells/ml. Surface staining with fluorochrome-conjugated antibodies (cat. nos and dilutions in Table SI) was performed for 20 min

on ice. Intracellular light chains were assessed after fixation/permeabilization (cat. no. 554722; BD Biosciences) using anti-cytoplasmic (c)κ-FITC and anti-cλ-PE. Internal negative controls were used for both fluorescence compensation and gating. T cells ($CD3^+CD19^-$) and B cells ($CD3^-CD19^+$) served as reciprocal negative controls, with compensation adjusted to achieve proper alignment of populations in all dot plots. Data acquisition was performed on a BD FACSCanto II (50,000-100,000 events/tube) and analyzed with FlowJo v10.8.1 (both from BD Biosciences). Gating employed CD45/SSC-A for initial lymphocyte discrimination, followed by CD19-positive B-cell enrichment for immunophenotypic characterization. The results revealed an increased lymphocyte proportion (60.4% of nucleated cells, P4), with CD19-positive cells (P9) accounting for ~72.2% of lymphocytes, suggesting the presence of abnormally mature B lymphocytes. Furthermore, the immunophenotypes of these abnormally mature B lymphocytes were analyzed. These cells exhibited strong positivity for cλ, CD19, CD20, CD79b and human leukocyte antigen-DR; partial positivity for CD23, CD25, CD27 and CD200; and negativity for cκ, CD5, CD10, CD22, CD38, CD103 and follicular mantle clone 7 (FMC7). Additionally, plasma cells exhibiting strong CD38 expression were identified, accounting for 0.30% of the cells (P10). Subsequent analysis of CD27 and CD38 expression levels in plasma cells revealed that the proportion of normal plasma cells was ~0.10% (P11), whereas abnormal plasma cells constituted ~0.20% (P12). Abnormal plasma cells showed strong expression of cλ, CD19, CD38 and CD138, partial expression of CD20 and CD27, and absence of cκ, CD5, CD10 or CD56 (Fig. 5).

Genetic testing plays a crucial role in accurately diagnosing WM and distinguishing it from other hematologic malignancies (2). IgM multiple myeloma (IgM-MM) often harbors the t(11;14) (q13; q32) translocation or other 14q32 [immunoglobulin heavy chain (IGH)] rearrangements, whereas the MYD88 L265P mutation is detected in >90% of WM cases (1,3,14,16). Accordingly, the MYD88 L265P mutation was detected by allele-specific polymerase chain reaction (AS-PCR) at Guangzhou Huayin Medical Laboratory Center (Guangzhou, China). The following primers were used: Forward 5'-CCT TGGCTTGCAGGTGC-3', reverse 5'-AGGATGCTG GGGAACTCTTT-3', and the following probes: Mutant (FAM-MGB) 5'-AAGCGACCGATCC-3', and wild-type (VIC-MGB) 5'-AAGCGACTGATCC-3'. Each 20-μl reaction contained 10 μl 2X qPCR Mix [with uracil-N-glycosylase (UNG)], 0.4 μl each primer (10 μM), 0.2 μl each probe (10 μM), 2-5 μl template DNA and nuclease-free water to a final volume of 20 μl. The thermal cycling conditions were as follows: 50˚C for 2 min, 95˚C for 10 min; 45 cycles of 95˚C for 15 sec and 60˚C for 60 sec. Fluorescence was acquired at FAM (mutant allele) and VIC/HEX (wild-type allele) channels at the end of each cycle. In this patient, genetic testing confirmed positivity for the MYD88 L265P mutation. AS-PCR showed a Cq value of 25.52 for the mutant allele and 23.03 for the wild-type allele (Fig. 6A). Subsequently, fluorescence *in situ* hybridization (FISH) was performed on bone marrow samples to detect the t(11;14) (q13;q32) translocation using the Vysis LSI IGH/cyclin D1 (CCND1) DF FISH Probe Kit (cat. no. 08L58-020; Abbott Laboratories, Inc.), following the manufacturer's instructions. FISH analysis, performed using an Olympus BX53 fluorescence microscope (Olympus Corporation), revealed a normal signal pattern in 199 out of 200 interphase nuclei (99.5%), with two copies each of CCND1 and IGH and no evidence of gene fusion, indicating the absence of the t(11;14) (q13;q32) translocation (Fig. 6B).

Treatment process and efficacy. Due to the patient showing serum IgM >40 g/l, complicated by hyperviscosity syndrome and cold agglutination, a stepwise therapeutic approach was chosen in accordance with the latest WM clinical practice guidelines (12). This strategy prioritized symptomatic relief of hyperviscosity with TPE followed by etiological chemotherapy targeting the underlying malignant lymphoplasmacytic proliferation. Initially, one cycle of TPE comprising five sessions was performed to rapidly mitigate acute hyperviscosity-related manifestations-a key and potentially life-threatening complication of WM-with fresh frozen plasma (FFP) as replacement fluid. Specifically, 2,000 ml FFP was administered in the first session, followed by 2,500 ml per session for each of the subsequent four sessions. During the first TPE session, the patient developed urticarial rash after FFP infusion, which resolved with temporary infusion cessation and intravenous dexamethasone (5 mg). Subsequent sessions were premedicated with intravenous dexamethasone (5 mg) 30 min prior to TPE, with no further allergic reactions. Upon completion of TPE, systemic chemotherapy with a bortezomib-dexamethasone regimen was initiated, consistent with frontline therapeutic recommendations for WM (1,3,12), to further control the disease and reduce tumor burden. The regimen was administered as follows: 2 mg of bortezomib was subcutaneously injected twice weekly (on days 1 and 4) for 2 consecutive weeks, and 10 mg of dexamethasone sodium phosphate was intravenously administered immediately after each bortezomib dose to enhance therapeutic efficacy and minimize adverse events. Concurrently, targeted supportive therapy was provided to manage other accompanying symptoms and improve the patient's treatment tolerance.

During one month of treatment, serial monitoring of clinical symptoms and core laboratory parameters were conducted, as shown in Table I. Before treatment, the patient presented with severe hyperviscosity syndrome and multiple organ damage, characterized by a markedly elevated serum IgM level (83.6 g/l), total protein (131 g/l) and globulin (92 g/l). Concurrently, the patient exhibited renal impairment (creatinine: 143 μmol/l; creatinine clearance rate: 45 ml/min; 24-UMTP: 1,018.8 mg/24 h), hypercalcemia (calcium: 3.15 mmol/l), and high tumor burden (β2-microglobulin: 6.16 mg/l, reference range: 1.3-3.0 mg/l). Immediately after TPE, the serum IgM level rapidly decreased by 48.5% to 43.04 g/l, with a concurrent reduction in total protein (from 131 to 99.3 g/l) and globulin (from 92 to 61 g/l), indicating immediate relief of hyperviscosity. Renal function also showed rapid improvement, with creatinine decreasing to 96 μmol/l, and hypercalcemia was corrected to 2.47 mmol/l within the normal range. At 1 month after bortezomib-based chemotherapy, sustained therapeutic effects were observed. The serum IgM level remained lower than before treatment (from 83.6 to 59.9 g/l)

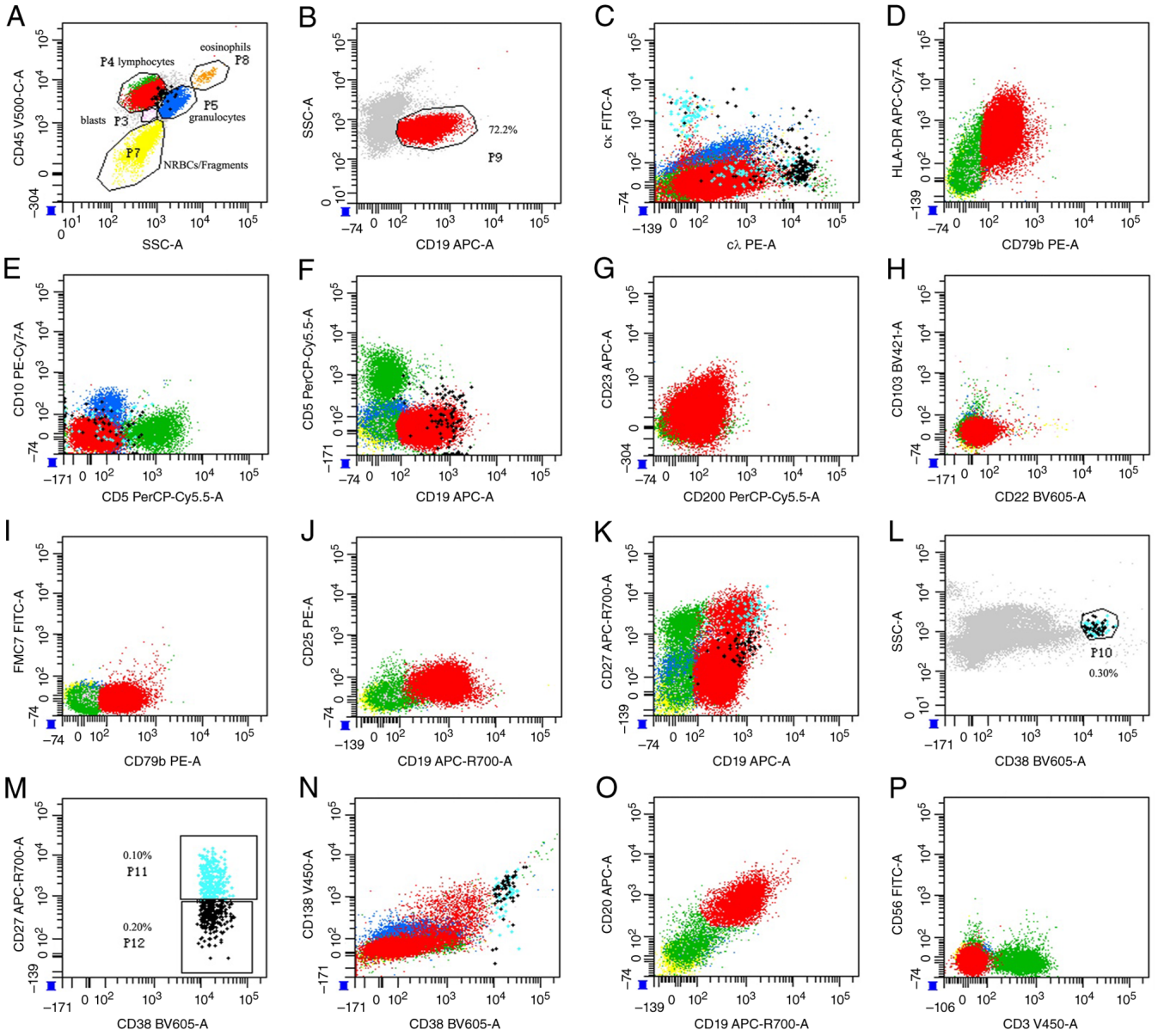

Figure 5. Immunophenotyping of bone marrow cells by flow cytometry. (A) CD45/SSC-A gating strategy: Blasts (P3), lymphocytes (P4), granulocytes (P5), NRBCs/fragments (P7), eosinophils (P8). (B) CD19/SSC-A: $CD19^+$ B cells comprised 72.2% of lymphocytes (P9). (C) cκ/cλ: Both light chains expressed. (D) HLA-DR/CD79b: Mature B-cell lineage confirmation. (E) CD10/CD5: Germinal center and T-cell marker evaluation. (F) CD5/CD19: $CD5^+CD19^+$ B-cell subset. (G) CD23/CD200: follicular vs. marginal zone phenotype. (H) CD103/CD22: $CD22^+CD103^-$/dim profile (excluding hairy cell leukemia). (I) FMC7/CD79b: Mature B-cell phenotype. (J) CD25/CD19: Activated B-cell subset ($CD19^+CD25^+$). (K) CD27/CD19: Naive ($CD27^-$) and memory ($CD27^+$) subsets. (L) SSC/CD38: Total plasma cells (P10: 0.30%). (M) CD27/CD38: Normal plasma cells (P11: 0.10%, $CD38^{++}CD27^+$) and abnormal plasma cells (P12: 0.20%, $CD38^{++}$CD27dim). (N) CD138/CD38: Plasmacytic differentiation. (O) CD20/CD19: Mature B cells ($CD19^+CD20^+$) vs. plasmacytic elements ($CD19^+$CD20dim). (P) CD56/CD3: Absence of T/NK-cell contamination. ++, bright positive; +, positive; -, negative; dim, partial expression/weak positive; SSC-A, side scatter-area; NRBCs, nucleated red blood cells; cκ, cytoplasmic κ light chain; cλ, cytoplasmic λ light chain; HLA-DR, human leukocyte antigen-DR isotype.

and the β2-microglobulin level dropped to <0.191 mg/l, demonstrating profound suppression of the underlying WM clone. Renal function was further improved, with creatinine normalized to 94 μmol/l and creatinine clearance rate increased to 74.32 ml/min. Hypercalcemia was completely corrected, with the calcium level stabilizing at 2.22 mmol/l. The 24-UMTP decreased from 1,018.8 to 867 mg/24 h, indicating ongoing recovery of renal injury.

Follow-up. After discharge, a structured follow-up plan was established, consisting of regular monthly visits with hematology and ophthalmology specialists to monitor disease activity. Follow-up evaluations included key indicators such as physical examinations, complete blood counts, serum biochemical tests and immunoglobulin quantification. However, follow-up was prematurely terminated after the first month (November 2023) because the patient required re-admission to the hospital for treatment of a pulmonary infection. Notably, the patient ultimately developed severe pulmonary infection and was admitted to the intensive care unit for management, thereafter progressing to multi-organ failure in the setting of profound systemic immunocompromise. Regrettably, in

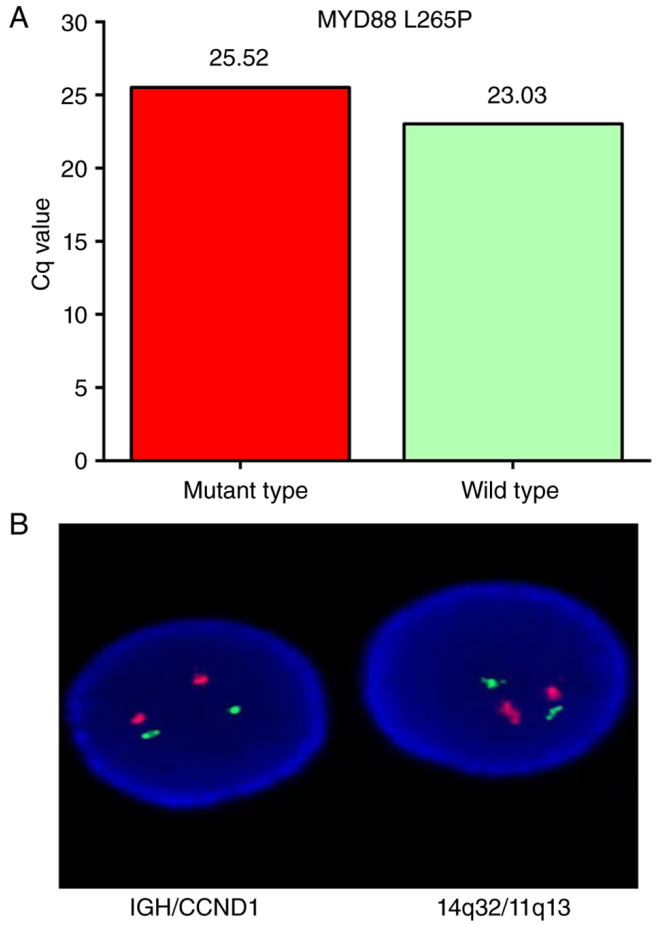

Figure 6. Genetic detection. (A) Allele-specific PCR detection of the MYD88 L265P mutation, positive. (B) Fluorescence *in vitro* hybridization detection of the 14q32/11q13 translocation via IGH/CCND1 probe (magnification, x1,000), negative. CCND1, cyclin D1; IGH, immunoglobulin heavy chain; MYD88, MYD88 innate immune signal transduction adaptor.

January 2025, the patient's family requested discharge and chose to withdraw active treatment.

Discussion

LPL/WM is a rare, indolent small B-cell lymphoma with plasma cell differentiation, accounting for <2% of all non-Hodgkin lymphoma cases (12). Pathologically, it is characterized by neoplastic proliferation of small B lymphocytes, plasmacytoid lymphocytes and plasma cells that overproduce monoclonal IgM, predominantly involving the bone marrow with less frequent lymph node or spleen involvement (17,18). Approximately 90-95% of LPL cases are classified as WM, whose typical clinical manifestations include anemia, hyperviscosity syndrome, renal impairment and less commonly organomegaly (1).

Cold agglutinin disease (CAD) is a relatively rare condition, primarily mediated by IgM (with IgG-mediated forms being rare), and serves as an important clinical indicator of underlying WM (6,19). In the present case, cold agglutination-induced laboratory interference served as the key diagnostic clue for WM. The patient's samples displayed classic temperature-dependent agglutination (gelation at 4˚C, liquefaction at 25˚C)-a hallmark manifestation of WM-related CAD, accompanied by peripheral blood erythrocyte rouleaux formation-findings that further confirmed pathological cold agglutination (6). This phenomenon is attributed to high-titer monoclonal IgM cold agglutinins (6). Notably, incubation of samples at 37˚C for 30 min resolved this interference, uncovering severe anemia (hemoglobin 54 g/l)-a manifestation attributable to the cold-agglutinating activity of monoclonal IgM, which recognizes specific erythrocyte antigen epitopes at temperatures <37˚C, and induces chronic hemolytic anemia, as previously reported (6,19-21). Thus, cold agglutination may serve as an early manifestation of IgM-secreting lymphoproliferative disorders, providing important clues for identifying potential patients.

Biochemical and immunoelectrophoretic findings supported clonal IgM secretion: Elevated total protein (131 g/l), globulin (92 g/l), inverted A/G ratio (0.42), marked serum IgM elevation (83.6 g/l), a dominant IgM-λ paraprotein (53.2% of γ-globulins) and urinary λ free light chains. While these findings are consistent with WM, they are not disease-specific-similar abnormalities may occur in IgM-type multiple myeloma (IgM-MM), IgM-type monoclonal gammopathy of undetermined significance (IgM-MGUS) and other B-LPDs (1,22). Therefore, a comprehensive approach combining clinical, laboratory, pathological, immunophenotypic and molecular testing data is required to make a definitive distinction.

Cytomorphology represents the fundamental histopathological basis for diagnosing hematological disorders (23). Peripheral blood smear in this patient showed erythrocyte rouleaux formation, lymphocytosis and numerous plasmacytoid lymphocytes. Bone marrow biopsy revealed extensive infiltration of B-lymphomatous cells (~80% of nucleated cells), 10% abnormal plasma cells, and the remaining 10% being residual normal hematopoietic cells, accompanied by focal collagenous fibrosis and large clusters of lymphocytes exhibiting plasmocytic differentiation. These findings, characterized by a B-cell lymphoproliferative process dominated by lymphoplasmacytic infiltration and marked suppression of normal hematopoiesis, are consistent with the pathological features of B-LPDs. Given the marked elevation of serum IgM-λ paraprotein in the patient, the primary diagnostic consideration centered on monoclonal IgM-secreting B-LPDs, specifically IgM-MM, WM and IgM-MGUS.

Rigorous differential diagnosis between WM, IgM-MGUS and IgM-MM is essential, as these entities differ fundamentally in clinical management and prognosis (1,24). According to the LPL/WM clinical practice guidelines, IgM-MGUS was readily ruled out in this patient (1,12). Defined as an asymptomatic, premalignant plasma cell disorder, IgM-MGUS requires serum monoclonal IgM <30 g/l, bone marrow lymphoplasmacytic infiltration <10% and the absence of organ or tissue-compromising manifestations or myeloma-defining end-organ damage. By contrast, the patient presented with a markedly elevated serum IgM level (83.6 g/l, far exceeding the 30 g/l threshold), extensive bone marrow lymphoplasmacytic infiltration (80% B-lymphomatous cells and 10% abnormal plasma cells) and overt clinical symptoms (severe anemia, hyperviscosity syndrome)-findings directly inconsistent with the asymptomatic, premalignant nature of IgM-MGUS.

Table I. Comparison of key indicators before and after treatment.

Index	Before treatment	After therapeutic plasma exchange	After chemotherapy	Reference range
Calcium, mmol/l	3.15	2.47	2.22	2.1-2.69
Total protein, g/l	131	99.3	98.3	63-82
Albumin, g/l	38.7	38.0	33.3	35-50
Globulin, g/l	92	61	65	24-35
IgG, g/l	6.05	10.75	7.61	8.6-17.4
IgA, g/l	0.55	1.59	0.62	1.0-4.2
IgM, g/l	83.6	43.04	59.9	0.3-2.2
Creatinine, μmol/l	143	96	94	58-110
Urea, mmol/l	8.0	8.62	8.31	3.6-9.5
Creatinine clearance rate, ml/min	45	/	74.32	>80
β2-microglobulin, mg/l	6.16	/	<0.191	1.3-3.0
24-UMTP, mg/24 h	1,018.8	/	867	50-80

24-UMTP, 24-h urinary total protein; IgM, immunoglobulin M.

Differentiating WM, a subtype of LPL, from the rare IgM-MM is clinically critical, with definitive distinction relying on integrated morphological, immunophenotypic, cytogenetic and molecular features (6,25-27). According to LPL/WM diagnostic guidelines (12), the typical immunophenotype of WM is CD19(+), CD20(+), sIgM(+), CD22(+), CD25(+), CD27(+), FMC7(+), CD23(-), CD5(-), CD10(-), usually CD38/CD138(+) and CD103(-), with 10-20% of patients also expressing CD5, CD10 or CD23 (27). Consistent with this guideline profile, the patient's bone marrow revealed a 60.4% lymphocyte population, of which 72.2% were abnormally mature B cells-highly expressing cλ, CD19 and CD20, partially expressing CD23, CD25 and CD27, and negative for CD5, CD10 and CD103. Abnormal plasma cells, accounting for 0.3% of nucleated cells, showed restricted cλ expression, high CD38, CD138 and CD19 expression, partial CD27 and CD20 expression, and negativity for CD5, CD10 and CD56. By contrast, IgM-MM is characterized by clonal plasma cells, high CD38 and CD138 expression, CD19 and CD45 negativity, and frequent osteolytic lesions (11,28). Gene testing provided decisive evidence to further distinguish these two entities: The MYD88 L265P mutation-a pathognomonic marker present in >90% of WM cases but rare in IgM-MM (<5%) and absent in IgM-MGUS (1,2,29,30), was detected in the patient. Additionally, t(11;14)(q13;q32) translocations, a type of IGH translocation frequently observed in IgM-MM (31,32), are uncommon in WM. Collectively, the patient's immunophenotype, positive MYD88 L265P mutation, negative 14q32 translocations and absence of pure plasma cell proliferation or osteolytic lesions firmly confirm WM and exclude IgM-MM, underscoring the clinical value of integrated testing for differentiating these rare IgM-secreting disorders.

For patients with high-risk WM with a serum IgM level of 83.6 g/l complicated by hyperviscosity syndrome and CAD, the core of treatment lies in balancing the relief of acute symptoms with long-term disease control. A guided strategy-initial TPE to rapidly alleviate life-threatening acute manifestations, followed by bortezomib and dexamethasone for etiological treatment-is fully aligned with current authoritative guidelines and clinical practice consensus (1,3,33).

TPE is universally recognized as the first-line emergency intervention for patients with WM with symptomatic hyperviscosity syndrome (34). Its mechanism involves the rapid clearance of large amounts of intravascular IgM, thereby promptly reducing serum viscosity and alleviating microcirculatory dysfunction (34). In this case, following TPE treatment, the patient's serum IgM level decreased from 83.6 to 43.04 g/l, accompanied by significant alleviation of hyperviscosity syndrome-related symptoms (dizziness, fatigue, blurred vision) and complete resolution of cold agglutination. This validates the exceptional efficacy of TPE in rapidly reducing IgM burden and reversing acute organ dysfunction. Notably, serum albumin remained stable during treatment (38.7 to 38.0 g/l), demonstrating the good safety profile of TPE when fresh frozen plasma is used as the replacement fluid, which effectively maintains plasma colloid osmotic pressure and prevents complications related to hypoalbuminemia (35).

Although TPE alleviates acute symptoms, it does not cure the disease, and IgM levels rebound rapidly. Therefore, immediate follow-up with systemic therapy is crucial. In the present study, a chemotherapy regimen centered on the proteasome inhibitor bortezomib was selected. This choice is consistent with the results of the WMCTG 05-180 clinical trial conducted by Treon *et al* (36), which demonstrated that the bortezomib-dexamethasone-rituximab regimen achieved an overall response rate as high as 96% in treatment-naive symptomatic patients with WM, significantly reducing tumor burden. Although rituximab was not administered in this case, single-agent bortezomib-dexamethasone still yielded significant, sustained efficacy. Following treatment, serum IgM was stably controlled at 59.9 g/l, the key tumor burden marker β2-microglobulin decreased markedly from 6.16

to <0.191 mg/l, and 24-UMTP declined from 1,018.8 mg to 867 mg. These findings confirm effective suppression of malignant lymphoplasmacytic proliferation and improvement in IgM-mediated renal injury (37), in line with reports that bortezomib induces durable remission in WM (37,38). Therefore, TPE combined with bortezomib and dexamethasone is an effective and safe strategy for patients with WM with severe hyperviscosity syndrome and CAD. Nevertheless, because IgM levels remained above normal after treatment, long-term follow-up is necessary, and subsequent addition of BTK inhibitors (e.g., ibrutinib, zanubrutinib) may be considered based on molecular typing and tolerability to achieve deeper remission.

Nevertheless, this case study has several limitations: i) As a single case report, it lacks statistical power and generalizability; ii) follow-up was prematurely terminated due to worsening symptoms, resulting in insufficient long-term data for efficacy and prognosis evaluation; and iii) mechanistic exploration is limited, and the causal relationships among related pathological factors remain unclear. Future studies should incorporate larger cohorts and in-depth molecular mechanistic investigations to enhance reliability and applicability.

In conclusion, in this case, cold agglutination-initially considered an analytical interference-served as a key diagnostic clue for IgM-secreting lymphoproliferative disorders. Integration of bone marrow morphology, immunophenotyping and MYD88 L265P mutation detection confirmed WM and excluded other IgM-secreting disorders, such as IgM-MM and IgM-MGUS. For patients with IgM-related cold agglutination, timely bone marrow examination, immunophenotyping and MYD88 L265P testing are crucial for accurate WM diagnosis. Early use of FFP as replacement fluid can rapidly relieve hyperviscosity syndrome, and subsequent chemotherapy can effectively control the underlying disease to improve clinical manifestations. This case provides valuable clinical experience for diagnosing and treating WM with atypical initial manifestations, particularly cold agglutination.

Acknowledgements

Not applicable.

Funding

The authors hereby express their gratitude for the support provided by the San Ming Project of Medicine in Shenzhen (grant no. szzysm202311020), the National Flagship Department Construction Project for Integrated Traditional Chinese and Western Medicine [National Administration of Traditional Chinese Medicine Comprehensive Integration Letter No. 221 (2024)] and the Team-based Medical Science Research Program (grant no. 2024YZZ07) for this research.

Availability of data and materials

The data generated in the present study may be requested from the corresponding author.

Authors' contributions

WZ and YX performed the patient's laboratory examinations, analyzed the data, and drafted the initial manuscript. ZY, LZ and XJ participated in collecting the patient's information and analyzing the data. TC and PM conceived the study, acquired funding, conducted the investigation, and participated in manuscript review and editing. All authors confirm the authenticity of all the raw data. All authors read and approved the final manuscript.

Ethics approval and consent to participate

This study was conducted in accordance with the Declaration of Helsinki and its amendments. According to Chinese laws and regulations, a case report does not constitute clinical research and thus does not require ethical review.

Patient consent for publication

Written informed consent for publication was obtained from the patient and their family. This case report includes all medical data, laboratory results, and clinical images collected during the patient's outpatient and inpatient care, with all personal identifiers removed to protect patient privacy.

Competing interests

The authors declare that they have no competing interests.

References

1. Gertz MA: Waldenström macroglobulinemia: 2025 update on diagnosis, risk stratification, and management. Am J Hematol 100: 1061-1073, 2025.
2. Treon SP, Xu L, Yang G, Zhou Y, Liu X, Cao Y, Sheehy P, Manning RJ, Patterson CJ, Tripsas C, *et al*: MYD88 L265P somatic mutation in Waldenström's macroglobulinemia. N Engl J Med 367: 826-833, 2012.
3. Treon SP, Sarosiek S and Castillo JJ: Diagnosis and management of Waldenstrom's macroglobulinemia. Hematol Oncol 43 (Suppl 2): e70071, 2025.
4. McMaster ML: The epidemiology of Waldenström macroglobulinemia. Semin Hematol 60: 65-72, 2023.
5. Zorlu T, Kayer MA, Okumus N, Ulaş T, Dal MS and Altuntas F. Challenges, difficulties, and delayed diagnosis of multiple myeloma. Diagnostics (Basel) 15: 1708, 2025.
6. Kozub A, Nasiek A, Bohun N, Bednarczyk M, Sędek Ł and Grosicki S: A rare combination: Cold agglutinin disease followed by Waldenström macroglobulinemia-A case of early treatment response. Diagnostics (Basel) 15: 2654, 2025.
7. Berentsen S: Diagnosis and management of cold agglutinin disease. Hematology Am Soc Hematol Educ Program 2025: 295-304, 2025.
8. Scarcella S, Tuccari G, Pizzimenti C, Scarcella SC, Martini M, Granata F, Germanò A, Ieni A and Tuccari G: Morphological, immunophenotypic and neuroradiological characteristics of primitive B-large cell diffuse lymphoma of the central nervous system: A retrospective cohort analysis. Oncol Lett 30: 433, 2025.
9. Hobbs M, Fonder A and Hwa YL: Waldenström macroglobulinemia: Clinical presentation, diagnosis, and management. J Adv Pract Oncol 11: 381-389, 2020.
10. Puig N, Ocio EM, Jiménez C, Paiva B, Miguel JFS and García-Sanz R: Waldenström's macroglobulinemia immunophenotype. In: Waldenström's Macroglobulinemia. Leblond V, Treon S and Dimoploulos M (eds). Springer International Publishing, Cham, pp21-34, 2017.

11. Trojani A, Beghini A, Bossi LE, Stefanucci MR, Palumbo C, Greco A, Frustaci A, Di Camillo B and Cairoli R: Mutational landscape of bone marrow CD19 and CD138 cells in Waldenström macroglobulinemia (WM) and IgM monoclonal gammopathy of undetermined significance (IgM MGUS). Cancer Med 13: e70525, 2024.
12. Kumar SK, Callander NS, Adekola K, Anderson LD Jr, Baljevic M, Baz R, Campagnaro E, Castillo JJ, Costello C, D'Angelo C, *et al*: Waldenström macroglobulinemia/lymphoplasmacytic lymphoma, version 2.2024, NCCN clinical practice guidelines in oncology. J Natl Compr Canc Netw 22: e240001, 2024.
13. Azoulay D, Tapuchi T, Ronen O, Akria L, Cohen HI, Surio C, Chepa SR, Eshel E, Zarfati M, Stemer G and Horowitz NA: Flow-cytometry assessment of DNA content and immunophenotyping of immune-cells in lymph-node-specimens as a potential diagnostic signature of aggressiveness in B-non-hodgkin lymphomas. Ann Hematol 103: 4203-4210, 2024.
14. Avet-Loiseau H, Garand R, Lodé L, Harousseau JL and Bataille R; Intergroupe Francophone du Myélome: Translocation t(11;14)(q13;q32) is the hallmark of IgM, IgE, and nonsecretory multiple myeloma variants. Blood 101: 1570-1571, 2003.
15. Craig FE and Foon KA: Flow cytometric immunophenotyping for hematologic neoplasms. Blood 111: 3941-3967, 2008.
16. Varettoni M, Arcaini L, Zibellini S, Boveri E, Rattotti S, Riboni R, Corso A, Orlandi E, Bonfichi M, Gotti M, *et al*: Prevalence and clinical significance of the MYD88 (L265P) somatic mutation in Waldenstrom's macroglobulinemia and related lymphoid neoplasms. Blood 121: 2522-2528, 2013.
17. Naderi N and Yang DT: Lymphoplasmacytic lymphoma and Waldenström macroglobulinemia. Arch Pathol Lab Med 137: 580-585, 2013.
18. Berentsen S, D'Sa S, Randen U, Małecka A and Vos JMI: Cold agglutinin disease: Improved understanding of pathogenesis helps define targets for therapy. Hemato 3: 574-594, 2022.
19. Berentsen S: New insights in the pathogenesis and therapy of cold agglutinin-mediated autoimmune hemolytic anemia. Front Immunol 11: 590, 2020.
20. Brodsky RA: Complement in hemolytic anemia. Blood 126: 2459-2465, 2015.
21. Berentsen S, Röth A, Randen U, Jilma B and Tjønnfjord GE: Cold agglutinin disease: Current challenges and future prospects. J Blood Med 10: 93-103, 2019.
22. Girard LP, Soekojo CY, Ooi M, Poon LM, Chng WJ and de Mel S: Immunoglobulin M paraproteinaemias. Cancers (Basel) 12: 1688, 2020.
23. Yadav DP, Kumar D, Jalal AS, Kumar A, Singh KU and Shah MA: Morphological diagnosis of hematologic malignancy using feature fusion-based deep convolutional neural network. Sci Rep 13: 16988, 2023.
24. Ghafoor B, Masthan SS, Hameed M, Akhtar HH, Khalid A, Ghafoor S, Allah HM, Arshad MM, Iqbal I, Iftikhar A, *et al*: Waldenström macroglobulinemia: A review of pathogenesis, current treatment, and future prospects. Ann Hematol 103: 1859-1876, 2024.
25. Chehal A, Taher A and Shamseddine A: IgM myeloma and Waldenstrom's macroglobulinemia: A distinct clinical feature, histology, immunophenotype, and chromosomal abnormality. Clin Lab Haematol 25: 187-190, 2003.
26. Cossarizza A, Chang HD, Radbruch A, Abrignani S, Addo R, Akdis M, Andrä I, Andreata F, Annunziato F, Arranz E, *et al*: Guidelines for the use of flow cytometry and cell sorting in immunological studies (third edition). Eur J Immunol 51: 2708-3145, 2021.
27. Sourdeau E, Boccon-Gibod C, Corneau A, Costopoulos M, Bravetti C, Armand M, Chapiro E, Nguyen-Khac F, Davi F, Blanc C, *et al*: Phenotypic profile of Waldenström macroglobulinaemia B-cells: Establishment of a diagnosis scoring system and clinico-biological correlations. J Cell Mol Med 29: e70620, 2025.
28. Riccardi F, Tangredi C, Dal Bo M and Toffoli G: Targeted therapy for multiple myeloma: An overview on CD138-based strategies. Front Oncol 14: 1370854, 2024.
29. Bagratuni T, Aktypi F, Theologi O, Sakkou M, Verrou KM, Mavrianou-Koutsoukou N, Patseas D, Liacos C, Skourti S, Papadimou A, *et al*: Single-cell analysis of $MYD^{88L265P}$ and $MYD88^{WT}$ Waldenström macroglobulinemia patients. Hemasphere 8: e27, 2024.
30. Yu X, Li W, Deng Q, Li L, Hsi ED, Young KH, Zhang M and Li Y: MYD88 L265P mutation in lymphoid malignancies. Cancer Res 78: 2457-2462, 2018.
31. Miura D, Narita K, Kuzume A, Tabata R, Terao T, Tsushima T, Kobayashi H, Abe Y, Kitadate A, Takeuchi M, *et al*: Clinical and prognostic impact of (11;14)(Q13;Q32) translocation on patients with multiple myeloma. Blood 134: 5507, 2019.
32. Fujishima T, Kobayashi T, Kobayashi I, Kitadate A, Kameoka Y and Takahashi N: Successful salvage therapy with pomalidomide, cyclophosphamide, and dexamethasone for IgM myeloma with t (11;14) and Dim CD38 expression refractory to daratumumab, lenalidomide, and dexamethasone. Intern Med 64: 3020-3026, 2025.
33. Grunenberg A and Buske C: How to manage waldenström's macroglobulinemia in 2024. Cancer Treat Rev 125: 102715, 2024.
34. Weaver A, Rubinstein S and Cornell RF: Hyperviscosity syndrome in paraprotein secreting conditions including waldenstrom macroglobulinemia. Front Oncol 10: 815, 2020.
35. Warner D, Duncan H, Gudsoorkar P and Anand M: Indications and complications associated with centrifuge-based therapeutic plasma exchange-a retrospective review. BMC Nephrol 26: 87, 2025.
36. Treon SP, Ioakimidis L, Soumerai JD, Patterson CJ, Sheehy P, Nelson M, Willen M, Matous J, Mattern J II, Diener JG, *et al*: Primary therapy of Waldenström macroglobulinemia with bortezomib, dexamethasone, and rituximab: WMCTG clinical trial 05-180. J Clin Oncol 27: 3830-3835, 2009.
37. Liu Z, Jiang S, Gu J, Liu H, Song G and Cao X: Bortezomib-based chemotherapy for patients with Waldenström macroglobulinemia: A single-center experience. Ann Hematol 102: 167-174, 2023.
38. Leblond V, Morel P, Dilhuidy MS, Leleu X, Soussain C, Leprête S, Dreyfus B, Dartigeas C, Mahé B, Anglaret B, *et al*: A phase II Bayesian sequential clinical trial in advanced Waldenström macroglobulinemia patients treated with bortezomib: Interest of addition of dexamethasone. Leuk Lymphoma 58: 2615-2623, 2017.